3-D Crustal Velocity Structure from Inversion of Local Earthquake Data in Attiki (Central Greece) Region

G. DRAKATOS, N. MELIS, D. PAPANASTASSIOU, V. KARASTATHIS, G.A. PAPADOPOULOS and G. STAVRAKAKIS
National Observatory of Athens – Institute of Geodynamics, P.O. Box 20048 GR 11810 Athens, Greece, E-mail: g.drakat@egelados.gein.noa.gr

Abstract. Three-dimensional velocity structure of the upper crust was determined by inversion of P-wave travel times in the region of Attiki Prefecture (Greece), located at the eastern part of the Greek mainland, which is traditionally considered as an area of low seismicity. An earthquake of Ms = 5.9 occurred there, on September 7, 1999, causing extensive damage in the metropolitan area of Athens. A two-step tomographic procedure was applied to investigate the 3-D crustal velocity structure. The data set consisted of travel time residuals of 466 very well located earthquakes. In order to improve the initial velocity model, before the inversion of the data, a 'minimum 1-D' initial velocity model was obtained and, therefore, for the first time a reliable velocity model for the region was derived. The results show that the velocity distribution is influenced rather from the geology than the seismotectonic regime of the region. At shallow depths (less than 4 km) the velocity increases gradually with respect to the depth without any sharp variation. On the contrary, the lateral variation of velocity seems to be affected from the geological regime of the region. The low velocities at this depth seem to be typical for sedimentary basins, like those of the investigated region. At deeper layers (larger than 5 km) a different picture is obtained where both the lateral and vertical velocity variations are sharply pronounced. At the depth of 8.5 km, the aftershock area is covered by relatively low velocities, while a region of higher velocity covers the central part of Attiki almost coinciding with the transition zone between the Pelagonian and Attico-Cycladic massifs. Finally, the influence of the geological regime is well expressed by a high velocity anomaly, which is predominant beneath the Palaeozoic and Mesozoic metamorphic basement of the investigated region.

Key words: crustal structure, seismic tomography, Greece, Attiki region.

1. Introduction

The region of Attiki, Central Greece (Figure 1), is traditionally considered as being of low seismicity. Only outside this region and close to its northern and western borders, sources of both historical and instrumental strong earthquakes exist all associated with a roughly N–S extensional (Figure 2) tectonic field (for more seismicity details we refer to the papers of Galanopoulos, 1953, 1960; Ambraseys, 1994; Ambraseys and Jackson, 1997; Papazachos and Papazachou, 1997; Papadopoulos *et al.*, 2000b). From social and economic points of view, however, the Attiki
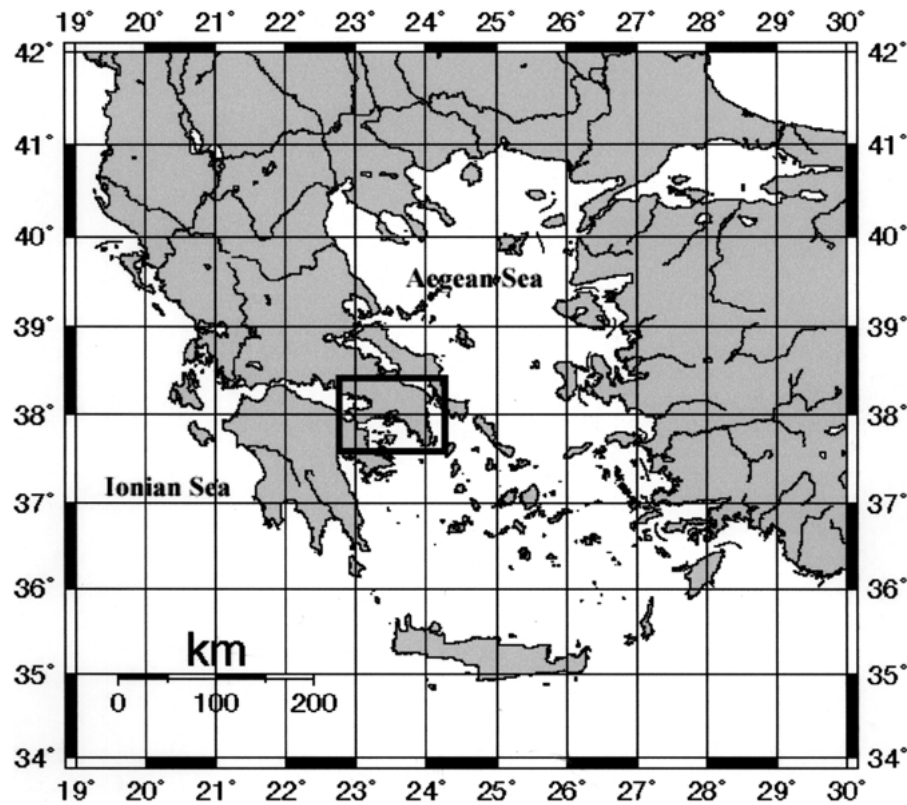
Figure 1. A map of Greece and the surrounding regions. The bold frame denotes the study region.

region is extremely important since the metropolitan area of Athens, the capital city of Greece, is situated in it. In fact, it is a region of dense population with nearly 40% of the total population of Greece, roughly 4 million people, along with most of the industrial, financial and administrative activities of the country being concentrated in this region.

On September 7, 1999 a moderate-to-strong earthquake (Ms = 5.9, 11:56:50.5 GMT) occurred at a small epicentral distance (D $\sim$ 18 km) from the historical center of Athens. The shock caused extensive damage with approximately one hundred cases of collapse of constructions in the northern and western part of the Athens area. A death toll of 143 was reported while the people rendered homeless during the first days after the earthquake was of the order of 100,000.

Fault plane solutions from near-field stations (Papadopoulos *et al.*, 2000a; Papadimitriou *et al.*, 2000; Papanastassiou *et al.*, 2000; Tselentis and Zahradnik, 2000; Voulgaris *et al.*, 2000) and from teleseismics (e.g., Harvard, USGS, Mednet) as well as geological field observations (Pavlides *et al.*, 1999) indicate that the main shock rupture was of normal type trending NNW–SSE and dipping SW.
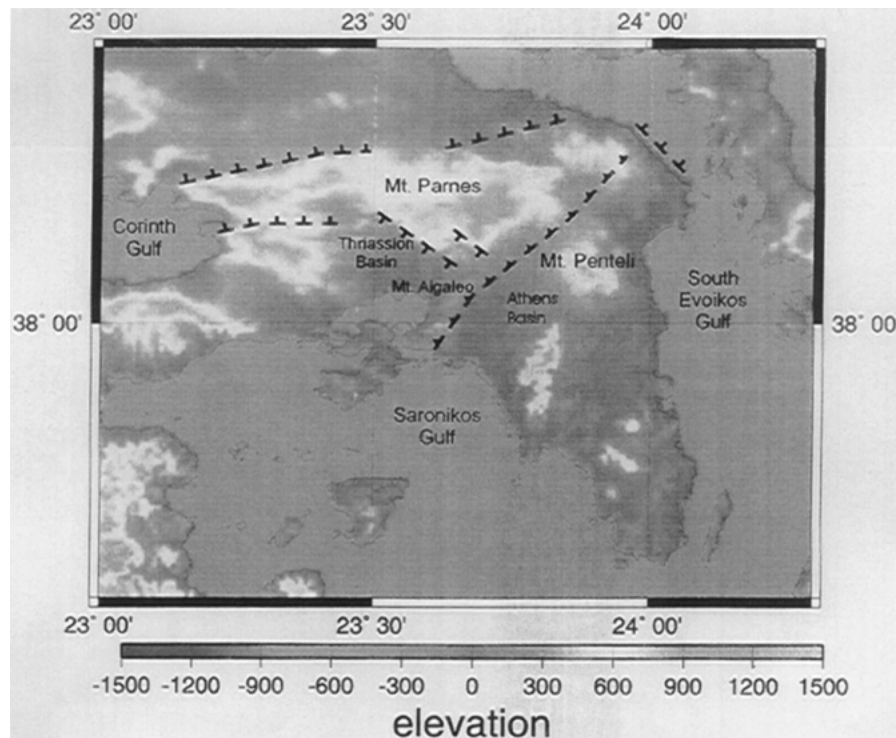
Figure 2. Simplified morphotectonic map of Attiki region redrawn by D. Papanastassiou from the geological map of IGME (Institute of Geology and Mineral Exploration) and from personal field observations.

The seismic moment, Mo, and fault radius, R, determined from the Greek digital stations are Mo = 7.13×10^{24} dyn cm and $R = 9.39$ km (Stavrakakis *et al.*, 2000).

The occurrence of the earthquake of 7th September 1999 initiated a great interest not only for a reassessment of the earthquake risk but also for understanding better the seismogenic processes in the Attiki region. It is beyond doubt that the knowledge of the fine crustal velocity structure is very important for making progress in that direction. However, the low seismicity and the subsequent lack of frequent operation of local seismograph networks in the Attiki region did not allow so far the investigation of its 3-D crustal structure. The little information that exists from tomography studies in Greece is only at regional scale (e.g., Spakman, 1986; Spakman *et al.*, 1988; Drakatos and Drakopoulos, 1991; Ligdas and Main, 1991; Papazachos *et al.*, 1995; Drakatos *et al.*, 1997; Papadopoulos, 1997; Melis and Tselentis, 1998). Most of them outline the predominant features of the Eastern Mediterranean region, like the subduction zone along the Hellenic arc, the South Aegean volcanic arc and the zone of seismic energy absorption in the central Aegean. Due to the parameterisation of the region, however, it is not possible to extract detailed information for more restricted regions. In the present study the 3-D crustal velocity structure of the Attiki region is investigated on the basis of
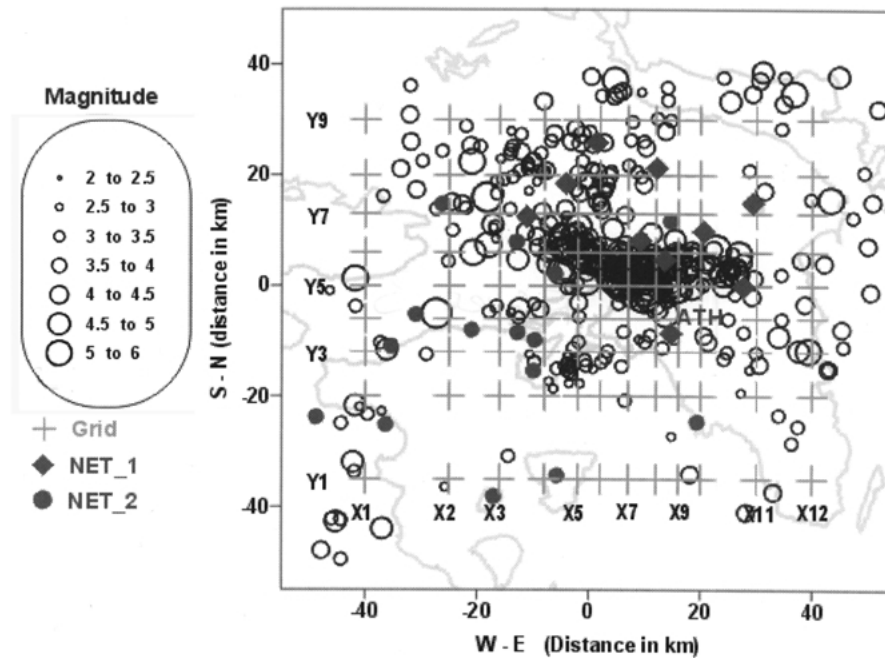
Figure 3. The 3D and non-uniform grid used in the present study (cross-lines). Open circles represent the epicentre distribution, while solid circles and squares represent stations of NET_1 and NET_2, respectively. ATH denotes the Athens station. The distances in W-E and S–N directions are measured (in km) from the center of the region (38°3′ N–23°33′ E).

data coming from two local seismic arrays. The first, NET-1, consisting of ten analog stations (Figure 3), was installed immediately after the 7 September 1999 earthquake for the monitoring of the aftershock activity. That network operated for about two months and more than 1500 aftershocks were recorded (Papadopoulos *et al.*, 2000a; Papanastassiou *et al.*, 2000). In addition, another local array, NET-2, of fifteen portable analog stations was operated for three months at the southern part of the Attiki region (Figure 3) during 1992 (DEPA, 1992).

The combined use of data from different seismic networks does not affect the results of studies concerning the structure of the Earth (e.g., Drakatos and Drako-poulos, 1991; Papazachos *et al.*, 1995). Moreover, the two networks were operated with instruments of the same type and, therefore, there are no problems with data compatibility. The data of the two seismic arrays were combined and the results obtained were utilized together to derive for the first time a reliable velocity model of the Attiki region as well as information about its crustal structure.

2. Regional Geological and Tectonic Setting

The region of Attiki has a complex geological structure. Its northern part consists of the non-metamorphic formations of the Pelagonian geotectonic zone, while its

southern part (Attica Unit) belongs to the Attico-Cycladic crystalline massif. The dominating tectonic feature is the overthrust between these two units composed of three successive thrusts (Rondoyanni *et al.*, 2000). More precisely, the Pelagonian zone is thrusted over the Attica unit along a southeast direction. The border line of the thrust is roughly located to the east of the southeastern mountain front of Parnes and Aegaleo (Figure 2).

The Attica unit is characterized as the autochthonous metamorphic basement of the Palaeozoic–Mesozoic age consisting of marbles and schists. Over this are found remnants of a tectonic cover. In the southern part of Attica, thrusted over the Attica unit is a system of phyllite, with intercalations of marbles, limestones, schists and quartzites. This system shows an imbricate structure and is of the Jurassic–Cretaceous age. The western part of Attica, which includes the mountains of Parnis and Aegaleo, belongs to the Pelagonian unit and consists of Paleozoic shales and phyllites, Triassic–Cretaceous limestones and Palaeocene flysh.

From a morphotectonic point of view the north and northwestern parts of Attica are characterized by a zone of normal faults which is the eastwards extension of the Corinth Gulf fault zone of almost E–W direction (Figure 2). Considerable earthquake activity has been observed along this fault zone during the instrumental and the historical period (see references in the Introduction).

3. Method

In order to investigate the three-dimensional crustal velocity structure of the region, the two-step tomography procedure proposed by Kissling *et al.* (1994) has been applied. The inverse problem of three-dimensional local earthquake tomography is formulated as a linear approximation to a non-linear function (Pavlis and Booker, 1983). In general, solutions are obtained by linearization with respect to a reference earth model (Aki and Lee, 1976; Nolet, 1978). Thus, the solutions obtained and the reliability estimates depend on the initial reference model. Inappropriate model may result in artifacts of significant amplitude. To overcome these problems, Kissling *et al.* (1994) proposed a two-step procedure to obtain 3-D tomographic results with minimal dependence of the reference model.

As a first step, the travel time data are jointly inverted to obtain a 1-D tomographic solution, together with revised hypocenter coordinates and station corrections. This model is called the "minimum 1-D model" (Kissling, 1988). The determination of this model is a trial and error process that ideally starts with the collection and selection of *a priori* information about the subsurface structure. Since this process can lead to ambiguous results, particularly when more than one *a priori* 1-D models have been established, several parameters which control the inversion need to be varied and the corresponding results need to be evaluated (Kissling *et al.*, 1994).

As a second step, the 3-D tomographic inversion is determined using the minimum 1-D model (Figure 4) as the starting model. In this step, the tomographic

technique initially introduced by Thurber (1983) and later improved by Eberhart-Phillips (1986; 1990) was applied. The method performs an iterative simultaneous inversion for 3-D velocity structure and hypocenter parameters using travel time residuals from local earthquakes. The velocity of the medium is parameterized by assigning velocity values at the intersections (grid points) of a non-uniform, three-dimensional grid. The spacing within the grid is selected by trying to have enough ray paths near each grid point so that its velocity may be well resolved. The spacing need not to be uniform throughout the study area. The velocity for a point along a ray path and the velocity partial derivatives are computed by linear interpolation between the surrounding grid points. Thus, the velocity solution will show gradation changes in velocity rather than the sharp discontinuities shown in typical refraction models or block-type parameterizations. As a ray tracing technique, the approximate ray tracing proposed by Thurber (1983) is used. This technique selects the ray paths as the arc with the fastest travel time out of a suite of circular arcs connecting the source and receiver. This very useful technique which performs very well for station to source distances less than 100 km (Thurber, 1983; Eberhart-Phillips, 1986; 1990), therefore is the most adequate to be applied in the case of the Attiki region.

4. Data Selection and Model Configuration

The resolution and the reliability of the tomographic results strongly depend upon the degree of intersection of crossing rays. This presumes a dense station network with good distribution all over the investigated area. In order to overcome this difficulty, a "quality sensitive" spatial filtering technique was applied. For this purpose a set of nodes has been considered in the investigated area, with grid spacing of 2 km in both horizontal and vertical directions and, therefore, a set of cubes was obtained. Within each cube a set of events was included. From each set the event with the maximum number of P-wave arrivals is included in the analysis, while the other events lying within the cube are removed. This procedure is repeated for all cubes and from an initial data set consisting of more than 1500 local earthquakes, the final data set is derived, including the arrival times of 466 very well located earthquakes (Figure 3). Each one of them is recorded by at least eight stations of the network. The relatively large number of events, concentrated in the central part of the region, outlines the aftershock area of 7th September earthquake (Figure 3).

For the implementation of the method, a set of nodes has been considered, in the area between 37.40°N–38.70° N and 22.70° E–24.50° E, distributed in seven horizontal layers at depths of 0.5,3, 4, 8.5, 12, 20 and 30 km, respectively. Each grid consists of twelve nodes and nine nodes in the E–W and N–S directions, respectively (Figure 3). The distance between two consequent nodes varies from 4 km to 10 km in both directions. Therefore, the array has an aperture of 80×65 km in E–W and N–S direction, respectively. The initial velocity values assigned at each horizontal plane of nodes are 4.50, 5.10, 5.60, 5.80, 6.00, 6.50, 7.00 and
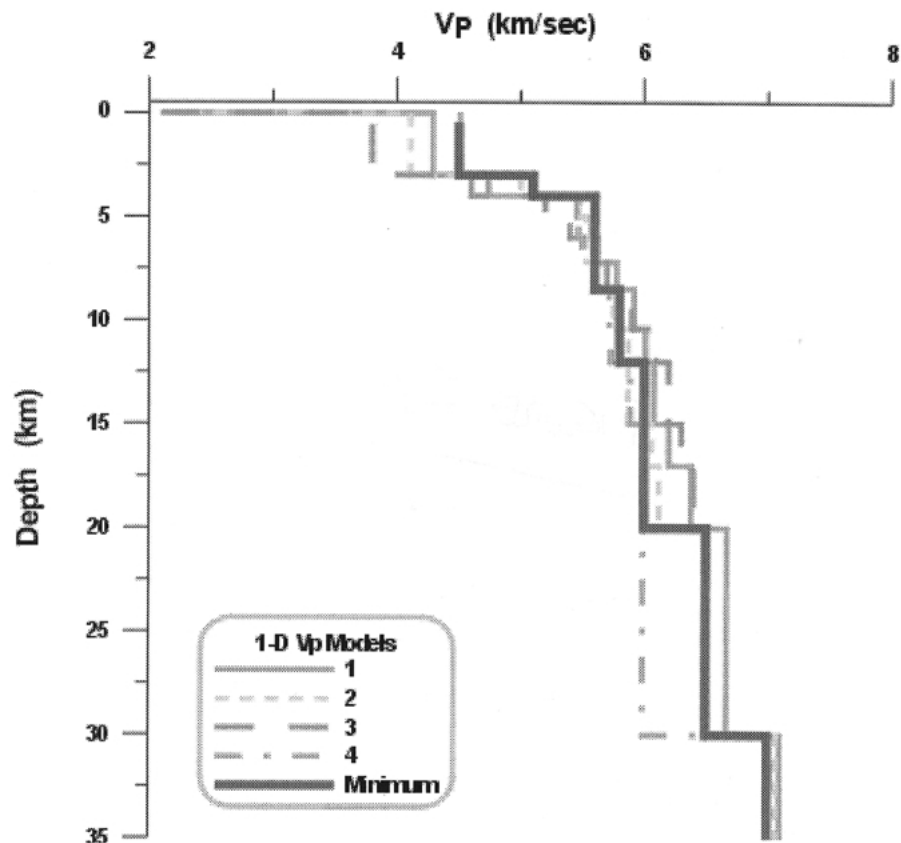
Figure 4. The lines (1–4) show the various velocity models used for the determination of the minimum 1-D model (bold line) used for the inversion.

8.00 km s^{-1}, respectively. The velocity model used is the "minimum 1-D model" (Figure 4 and Table I), which has been obtained following the procedure proposed by Kissling *et al.* (1994). A total number of 3848 P-arrivals was used. Some of the events were located outside the modeled area. The inclusion of earthquakes and/or stations falling outside the modeled area, that is the tomography box, is necessary to improve the ray path distribution within the modeled area. If only events and stations located within the modeled area were included, the quality of hypocenter location and resolution of velocity would be significantly reduced. However, in interpreting the results it should be remembered that the peripheral velocity grid-points include ray paths from the surrounding area.

A relocation of the events was made before the application of the inversion procedure. With the purpose to achieve the best depth determination, in the relocation step we included not only P-wave but also S-wave arrivals. Totally, 6810 arrivals (3848 P-wave and 2962 S-wave readings) were considered. The data set has been inverted three times to get a stable solution.

Table I. Minimum 1-D Model

Depth (km)	Velocity (km s^{-1})
0.0	4.5
3.0	5.1
4.0	5.6
8.5	5.8
12.0	6.0
20.0	6.5
30.0	7.0

5. Results

In Table I the 1-D velocity model obtained is presented. After the final relocation of the events the RMS values were improved significantly and most of the events have RMS value varying from 0.25 to 0.35 s (Figure 5). The magnitude and focal depth distributions, as received after the relocation, are also shown in Figure 5. The results of the inversion are displaced in Figures 6 and 7 in terms of velocity values at each node and only for the well resolved layers, while Figure 7 shows the velocity distribution, in a uniform color scale, along the cross-sections (grid lines) of Figure 3. Several parameters, like the number of hits at each block, the sum of derivatives etc., can be used to check the reliability and stability of the solution. The best of them is the diagonal element of resolution matrix. The resolution and hence the reliability and the stability of the solution strongly depend upon the degree of intersection of crossing rays. This presumes a dense station network with good distribution all over the investigated area. Despite the relatively low number of stations, the resolution values were high due to the fine distribution of the selected events and the small area of the investigated region. As a result, a large number of crossing rays pass from the grid points where the velocity values are calculated. Finally, the epicentre distribution with respect to the depth (Figure 8) is derived.

6. Interpretation – Discussion

The restricted area of the investigated region, measuring only about 80 × 65 km, along with that the focal depths of the earthquake events are almost confined within the upper 25 km of the crust (Figure 8), make the Moho discontinuity to be poorly resolved. Therefore, a Moho depth of about 30 km was considered as an *a priori* information. This assumption is compatible with the results of previous geophysical and tomographic investigations, which determine the Moho discontinuity at the investigated region, at the depth of about 28 km (Makris, 1978; Drakatos and Drakopoulos, 1991; Papazachos, 1993; Papazachos *et al.*, 1995; Drakatos *et al.*, 1997). Moreover, the above mentioned investigations show that there is a strong
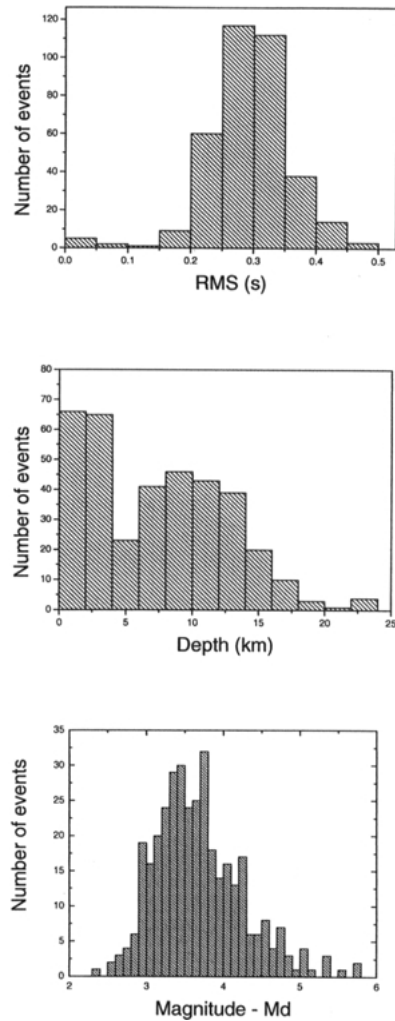
Figure 5. Frequency distribution of the RMS, the focal depth of earthquakes after relocation as well as of the earthquake magnitude distribution.

correlation between the surface geology and the velocity distribution in the upper crust, to a mean depth of 15 km. This is also shown from the results of the present study.

At shallow depths, less than 4 km, a gradual vertical increase of the velocity is observed, without any sharp variation (Figure 7). On the contrary, the lateral variation of the velocity seems to be affected from the geological regime of the region. More precisely, low velocities are predominant in the sedimentary basins of Thriassio and Athens, while higher velocities are detected beneath the mountains of Parnes and Penteli (Figures 2, 6 and 7). The low velocities at this depth seem to be typical for sedimentary basins like those characterizing the investigated region.
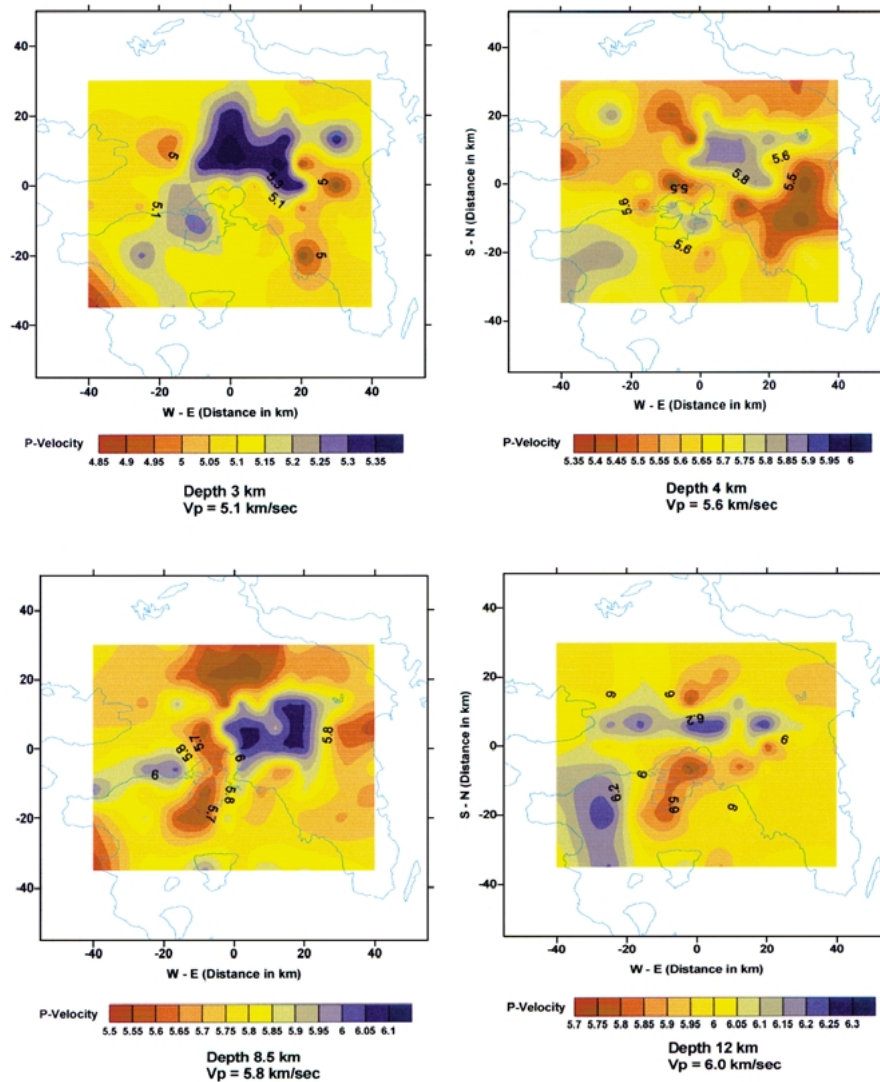
Figure 6. Velocity distribution derived after the inversion for the well resolved layers. The depth (in km) and the initial velocity value (in km s^{-1}) for each layer are also shown.

At the depth of 4 km, the lateral variation is rather small being less than 10% with its value ranging from 5.40 to 5.90 km s^{-1}. In general, the sedimentary layer in the eastern Mediterranean region shows a rather high complexity, due to its limited extension mainly in the neogene basins (Papazachos, 1993).

At layers deeper than 5 km, the picture changes drastically and both lateral and vertical velocity variations are sharply pronounced. At the depth of 8.5 km (Figures 6 and 7), the area of the 1999 main shock is covered by relatively low velocities. This is a consequence of the aftershock zone being located in the hanging wall of
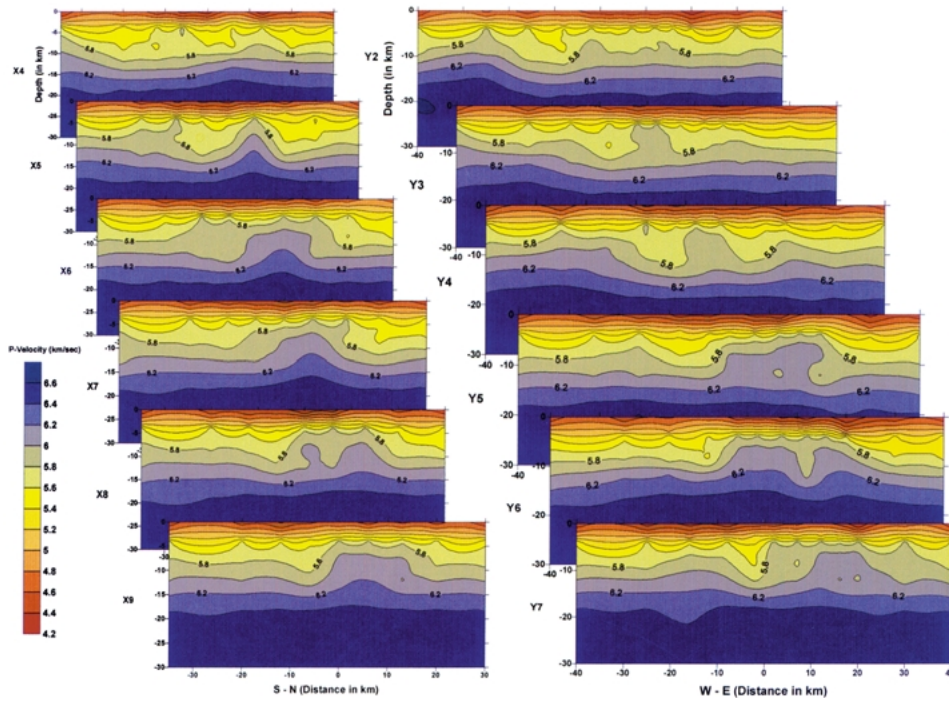
Figure 7. Vertical variation of the velocity (in km s^{-1}) along the cross sections shown in Figure 3. In both directions, the distances are measured (in km) from the center of the region (38°3′ N–23°33′ E).
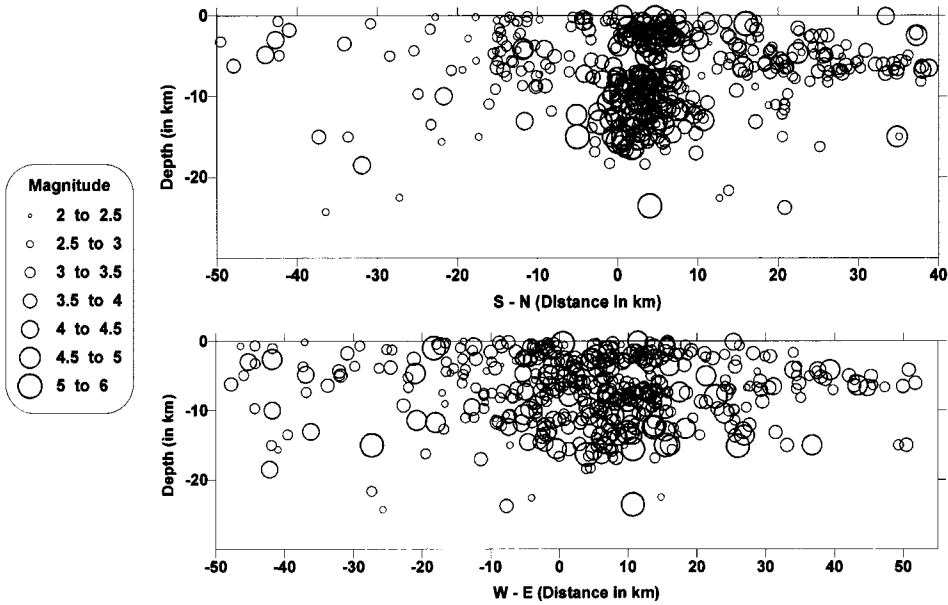

Figure 8. Epicenter distribution with respect to the depth along the S–N and W–E directions.

the fault and, therefore, being disconnected from the fault itself. The high fracturing of the region, and hence the existence of low velocities, can also be derived from the distribution of the events with respect to the depth (Figure 8).

At the same depth, a region of higher velocity covers the central part of Attiki almost coinciding with the transition between the Pelagonian and Attico-Cycladic massifs. In addition, relatively low velocities are predominant at the Saronikos Gulf, as a result of its sedimentary character, while a well-pronounced high velocity zone prevails in the region beneath the Aegaleo, Parnes and Penteli mountains (Figures 6 and 7). Finally, the influence of the geological regime in the velocity distribution is expressed by a higher velocity anomaly, which starts from a depth of about 12 km and is well pronounced up to the depth of 5 km (Figure 7). This anomaly is in good correlation with the Palaeozoic and Mesozoic metamorphic basement of the investigated region.

Acknowledgments

References

Aki, K. and Lee, W. H. K.: 1976, Determination of three-dimensional velocity anomalies under a seismic array using first P arrival times from local earthquakes, 1. A homogeneous initial model. *J. Geophys. Res.* **81**, 4381–4399.

Ambraseys, N. N.: 1994, Material for the investigation of the seismicity of Central Greece, In: P. Albini and A. Moroni (eds), *Historical Investigation of the Seismicity of European Earthquakes*, **2**, 1–10.

Ambraseys, N. N. and Jackson, A.: 1997, Seismicity and strain in the Gulf of Corinth (Greece) since 1694, *J. Earth. Eng.* **1**, 433–474.

DEPA: 1992. Fault evaluation study for Revithoussa island LNG Plant and nearby area, Greece.

Drakatos, G. and Drakopoulos, J.: 1991. 3D velocity structure beneath the crust and upper mantle of the Aegean Sea region, *Pure and Appl. Geophysics* **135**, 401–420.

Drakatos, G., Karantonis, G., and Stavrakakis, G.: 1997. P-wave crustal tomography of Greece with the use of an accurate two-point ray tracer, *Annali di Geofisica* **XL**(1), 25–36.

Eberhart-Philips, D.: 1986, Three-dimensional velocity structure in Northern California coast ranges from inversion of local earthquake arrival times, *Bull. Seism. Soc. Am.* **76**(4), 1025–1052.

Eberhart-Philips, D.: 1990, Three-dimensional P and S velocity structure in the Coalinga region, *California. J. Geophys. Res.* **95**, 15343–15363.

Galanopoulos, A. G.: 1953, Katalog der Erdeben in Griechland fur die Zeit von 1879 bis 1892, *Ann. Geol. Pays Hellen.* **5**, 144–229.

Galanopoulos, A. G.: 1960, Greece: A vatalogue of shocks with Io >VI or M > 5 for the years 1801–1958. Seism. Lab. Univ. Athens.

Kissling, E.: 1988, Geotomography with local earthquake data. *Rev. Geophys.* **26**, 659–698.

Kissling, E., Ellsworth, W. L., Eberhart-Phillips, D., and Kradolfer. U.: 1994, Initial reference models in local earthquake tomography, *J. Geophys. Res.* **99**(B10), 19,635–19,646.

Ligdas, C. N. and Main, I. G.: 1991, On the resolving power of tomographic images in the Aegean area, *Geophys. J. Int.* **107**, 197–203.

Makris, J.: 1978, The crust and upper mantle of Aegean region from deep seismic soundings, *Tectonophysics* **46**, 289–264.

Melis, N. and Tselentis, G-A.: 1998, 3-D P-wave velocity structure in western Greece determined from tomography using earthquake data recorded at the University of Patras Seismic Network (PATNET), *Pure Appl. Geophys.* **152**, 329–348.

Nolet, G.: 1978, Simultaneous inversion of seismic data, *Geophys. J. Roy. Astron. Soc.* **55**, 679–691.

Papadimitriou, P., Kaviris, G., Voulgaris, N., Kassaras, I., Delibasis, N., and Makropoulos, K.: 2000, The September 7, 1999 Athens earthquake sequence recorded by the CORNET network: Preliminary results of source parameters determination of the main shock, *Ann. Geol. Pays Hellen.* **38**(B), 29–40.

Papadopoulos, G. A.: 1997, On the interpretation of large-scale seismic tomography images in the Aegean sea area, *Annali di Geofisica* **XL**(1), 37–42.

Papadopoulos, G. A., Drakatos, G., Papanastassiou, D., Kalogeras, I., and Stavrakakis, G.: 2000a, Preliminary results about the catastrophic earthquake of 7 September 1999 in Athens, Greece, *Seism. Res. Lett.* **17**(3), 318–329.

Papadopoulos, G. A., Vassilopoulou, A., and Plessa, A.: 2000b, A catalogue of historical earthquakes for central Greece: 480 B.C.–1910 A.D.. Institute of Geodynamics, National Observatory of Athens, Publ. No 11.

Papanastassiou, D., Stavrakakis, G., Drakatos, G., and Papadopoulos, G.: 2000, The Athens, September 7, 1999, Ms = 5.9, earthquake: first results on the focal properties of the main shock and the aftershock sequence, *Ann. Geol. Pays Hellen.* **38**(B), 73–88.

Papazachos, C.: 1993, Determination of crustal thickness by inversion of travel times with an application in the Aegean area, *Proc. 2nd Cong. Hell. Geophys. Union, 5–7 May 1993*, Florina (Greece), Vol. II, pp. 483–491.

Papazachos, B. C. and Papazachou, K.: 1997, *The Earthquakes of Greece*, Zitti Publ., Thessaloniki, 304 pp.

Papazachos, C. B., Hatzidimitriou, P. M., Panagiotopoulos, D. G., and Tsokas, G. N.: 1995, Tomography of the crust and upper mantle in southeast Europe, *J. Geophys. Res.* **100**(B7), 12405–12422.

Pavlides, S., Papadopoulos, G. A., and Ganas, A.: 1999, The 7th September, 1999 unexpected earthquake of Athens: Preliminary results on the seismotectonic environment, *Proc. 1st Conference Advances in Natural Hazard Mitigation: Experiences from Europe and Japan*, Athens 3–4 November, 1999, pp. 80–85.

Pavlis, G. L. and Booker, J.: 1983, A study of importance on nonlinearity in the inversion of earthquake arrival time data for velocity structure, *J. Geophys. Res.* **88**, 5047–5055.

Rondoyanni, Th., Mettos, A., Galanakis, D., and Georgiou, Ch.: 2000, The Athens earthquake of September 7, 1999: its setting and effects, *Ann. Geol. Pays Hellen.* **38**(B), 131–144.

Stavrakakis, G. N., Chouliaras, G., and Panopoulou, G.: 2000, Seismic source parameters for the Athens earthquake on September 7, 1999, from a new telemetric broad band seismological network in Greece, *Ann. Geol. Pays Hellen.* **38**(B), 15–28.

Spakman, W.: 1986, Subduction beneath Eurasia in connection with the Mesozoic Tethys, *Geol. Mijnbow.* **65**, 145–153.

Spakman, W., Wortel, M. J. R., and Vlaar, N. J.: 1988. The Hellenic subduction zone: a tomographic image and its dynamic implications, *Geophys. Res. Lett.* **15**, 60–63.

Thurber, C. H.: 1983, Earthquake locations and three-dimensional structure in the Coyote Lake area, Central California, *J. Geophys. Res.* **88**, 8226–8236.

Tselentis, G-A. and Zahradnik, J.: 2000, Aftershock monitoring of the Athens earthquake of 7 September 1999, *Seism. Res. Lett.* **71**, 330–337.

Voulgaris, N., Kassaras, I., Papadimitriou, P., and Delibasis, N.: 2000, Preliminary results of the Athens September 7, 1999 aftershock sequence, *Ann. Geol. Pays Hellen.* **38**(B), 51–62.